# Using Characteristic Multiplier Loci to Predict Bifurcation Phenomena and Chaos—A Tutorial

Laurent Duchesne

*Abstract*—**This paper presents a tutorial on the interpretation and applications of characteristic multipliers (CM's). It gives a definition of this concept and its applications using Chua's circuit as a vehicle of illustration. Two basic bifurcation routes to chaos are studied: period doubling and transition to torus.**

## I. Introduction

The purpose of this paper is to explain the meaning of the concept of characteristic multiplier (CM) for dynamical systems and use it to predict various bifurcation phenomena. We will use Chua's circuit [1] to illustrate the physical interpretation and applications of the *CM loci* for predicting the onset of two standard routes to chaos: namely, the *period-doubling route* and the *quasi-periodic route*, corresponding to the birth of a *torus*, and its eventual breakdown to chaos.

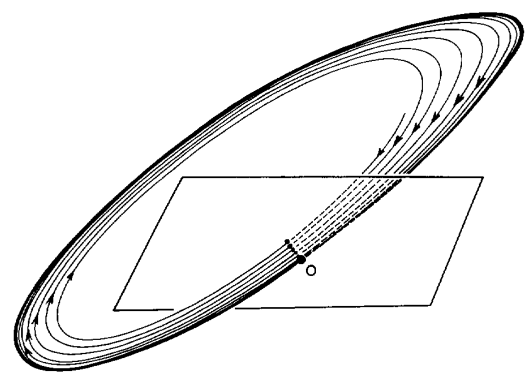

Fig. 1. A limit cycle obtained with $\alpha = 7.1$, $\beta = 100/7$, $a = -8/7$, and $b = -5/7$ in the dimensionless Chua's equation. Trajectories originating *near* the fixed point $x^*$ will necessarily return to points near $x^*$, thereby defining a mapping $\boldsymbol{P}$, valid in a *small* neighborhood of $x^*$.

## II. Definition of the Characteristic Multiplier

### 2.1. Autonomous Systems

For pedagogical reasons, we will consider only the class of autonomous continuous-time dynamical systems defined by the state equation:

$$\dot{\boldsymbol{x}} = \boldsymbol{f}(\boldsymbol{x}); \qquad \boldsymbol{x}(t_0) = \boldsymbol{x}_0$$

where $\dot{\boldsymbol{x}} = d\boldsymbol{x}/dt$, $\boldsymbol{x}(t)$ is the state at time $t$. To show explicitly the dependence on the initial condition, the solution $x = \Phi(t)$ of the state equation is often written in the form $\Phi_t(x_0)$ and read as the flow from $x_0$ evaluated at time $t$.

As a vehicle of illustration, we will use throughout this paper the autonomous system describing Chua's circuit [1]–[3], namely, the dimensionless Chua's equation:

$$\left\{\begin{array}{l} \dot{x} = \alpha(y - x - f(x)) \\ \dot{y} = x - y + z \\ \dot{z} = -\beta y \end{array}\right\}$$

where $f(x) = bx + \frac{1}{2}(a - b)(|x + 1| - |x - 1|)$.

### 2.2. Poincaré Map

Consider an autonomous system with a limit cycle $\Gamma$. Let $\boldsymbol{x}^*$ be a point on the limit cycle and let $\Sigma$ be a hyperplane transversal (i.e., perpendicular) to $\Gamma$ at $\boldsymbol{x}^*$. The trajectory emanating from $\boldsymbol{x}^*$ will hit $\Sigma$ at $\boldsymbol{x}^*$ in $T$ seconds, where $T$ is the minimum period of the limit cycle. Due to the continuity of $\Phi_t$ with respect to the initial condition, trajectories starting on $\Sigma$ in a sufficiently close neighborhood of $\boldsymbol{x}^*$ will, in approximately $T$ seconds, intersect $\Sigma$ in the vicinity of $\boldsymbol{x}^*$. Hence, $\Phi_t$ and $\Sigma$ define a mapping $\boldsymbol{P}$ of some neighborhood of $\boldsymbol{x}^*$ onto a neighborhood of $\boldsymbol{x}^*$. The function $\boldsymbol{P}$ is called a *Poincaré map* of the autonomous system. Since $\boldsymbol{P}(\boldsymbol{x}^*) = \boldsymbol{x}^*$, the point $\boldsymbol{x}^*$ is called a *fixed point* of $\boldsymbol{P}$. See Fig. 1.

### 2.3. Characteristic Multiplier

Consider a system with a limit cycle and a Poincare map $\boldsymbol{P}$ associated with this cycle at some convenient (arbitrarily chosen) fixed point $\boldsymbol{x}^*$ located on this cycle. The local behavior of the map near $\boldsymbol{x}^*$ is determined by linearising the map at $\boldsymbol{x}^*$. In particular, the linear map

$$\delta \boldsymbol{x}_{k+1} = D\boldsymbol{P}(\boldsymbol{x}^*)\, \delta \boldsymbol{x}_k$$

where $D\boldsymbol{P}(\boldsymbol{x}^*)$ denotes the Jacobian matrix of $\boldsymbol{P}$ evaluated at $\boldsymbol{x} = \boldsymbol{x}^*$, governs the evolution of the perturbation $\delta \boldsymbol{x}_0$ in a neighborhood of the fixed point $\boldsymbol{x}^*$. The eigenvalues of $D\boldsymbol{P}(\boldsymbol{x}^*)$ are called *CM's* of the periodic solution.

To illustrate the physical meaning of the CM's associated with a limit cycle, the three waveforms $[x(t), y(t), z(t)]$ associated with three different limit cycles from Chua's circuit are shown in Figs. 2(a), 3(a), and 4(a), respectively. For each

Manuscript received April 25, 1993; revised June 22, 1993. This paper was recommended by Guest Editor L. O. Chua.

L. Duchesne is with Ecole Nationale Superieure de l'Aeronautique et de l'Espace, Toulouse, France.

IEEE Log Number 9211606.

TABLE I
DATA FOR PLOTTING THE CM LOCI IN FIG. 5

| | $\alpha$ | CM 1 | CM 2 | normalized period | remarks |
|---|---|---|---|---|---|
| 1 | 6.79766 | 0.996932 | 0.250806E-2 | 1 | real |
| | 7.07 | 0.018047 | 0.5132 | 1 | |
| | 7.2 | 0.343147 | 0.030439 | 1 | |
| 2 | 7.3419 | 0.103884 | | 1 | double real root (real to complex) |
| | 7.4 | 0.0725047 | ± j 0.0796783 | 1 | complex-conjugate |
| 3 | 7.5196 | 0 | ± j 0.110039 | 1 | pure imaginary |
| | 7.6 | −0.0513406 | ± j 0.0987473 | 1 | |
| 4 | 7.69118 | −0.112058 | | 1 | complex to real |
| | 7.8 | −0.342601 | −0.0376925 | 1 | |
| | 8 | −0.677317 | −0.0195673 | 1 | |
| 5 | 8.1752 | −1.00008 | −0.0134305 | 1 | period 1 unstable |
| | 8.2 | 0.803608 | 0.00217002 | 2 | |
| 6 | 8.29172 | 0.0123856 | ± j 0.205512E-3 | 2 | real to complex |
| 7 | 8.29449 | 0 | ± j 0.0123010 | 2 | pure imaginary |
| 8 | 8.2973 | −0.000965628 | −0.0157617 | 2 | complex to real |
| | 8.35 | −0.515111 | −0.00273908 | 2 | |
| 9 | 8.3993 | −1.00103 | −0.131247E-3 | 2 | period 2 unstable |
| 10 | 8.422870 | 0.751798E-4 | 0.250407E-3 | 4 | real to complex |
| 11 | 8.422876 | 0 | ± j 0.136543E-3 | 4 | pure imaginary |
| 12 | 8.422883 | −0.115728E-3 | −0.168410E-3 | 4 | complex to real |
| 13 | 8.44457 | −0.999672 | −0.120952E-5 | 4 | period 4 unstable |
| 14 | 8.45419 | −0.999279 | 0.666406E-4 | 8 | period 8 unstable |

of these limit cycles, we have calculated the CM's using the program INSITE [4].

The CM's associated with Fig. 2(a) are *real* and *positive* ($\lambda_1 = 0.021437$, $\lambda_2 = 0.49638$) and both lie inside the unit circle. The two associated eigenvectors are shown in Fig. 2(b) along with several points corresponding to successive iterates of the Poincare map. Observe that these iterates lie near the upper eigenvector since the first eigenvalue $\lambda_1 = 0.021437$ is much smaller than the second eigenvalue $\lambda_2 = 0.49638$. The exponential convergence of the iterates to the fixed point (labelled as $\boldsymbol{O}$) in Fig. 2(b) can be correlated with the *exponential* envelope in the transient waveforms which converges to a *periodic* waveform corresponding to the fixed point $\boldsymbol{x}^*$, which we labeled in Fig. 2(b) as $\boldsymbol{O}$ for simplicity.

The CM's associated with Fig. 3(a) are *real* and *negative* ($\lambda_1 = -0.017352$, $\lambda_2 = -0.79418$) and both lie inside the unit circle. The two associated eigenvectors are shown in Fig. 3(b) along with several points corresponding to successive iterates of the Poincaré map. Observe that these iterates lie near the upper eigenvector for the same reason as in Fig. 2(b) ($|\lambda_1| \ll |\lambda_2|$). However, because the signs of $\lambda_1$ and $\lambda_2$ are both negative, the iterates in fig. 3b oscillate alternately about 0 while converging exponentially to the fixed point $\boldsymbol{O}$. This convergence phenomena can again be correlated with the transient waveforms in Fig. 3(a).

The CM's associated with Fig. 4(a) are complex-conjugate numbers lying inside the unit circle ($\lambda_1 = 0.766259 + j0.584179$, $\lambda_2 = 0.766259 - j0.584179$). Observe that the corresponding iterates of the Poincaré map shown in Fig. 4(b) now "spirals" into the fixed point $\boldsymbol{O}$. The corresponding interpretation in the transient waveforms is clearly depicted in Fig. 4(a).

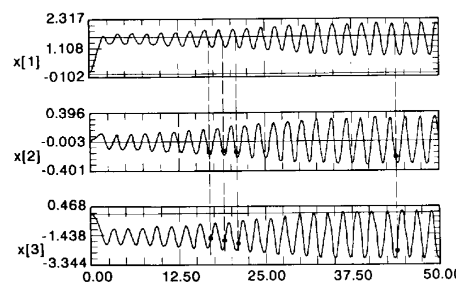


(a)

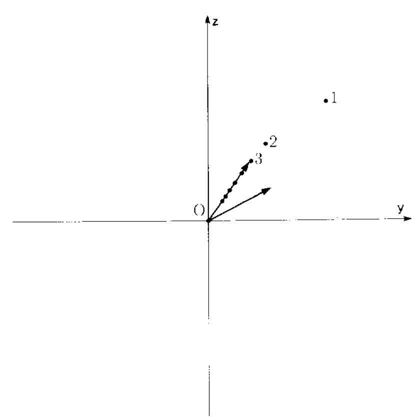


(b)

Fig. 2. (a) Waveforms associated with a stable limit cycle from Chua's circuit obtained with $\alpha = 7.1$, $\beta = 100/7$, $a = -8/7$, and $b = -5.7$. (b) Eigenvectors associated with two positive eigenvalues of the Poincaré map of the stable limit cycle of Fig. 2(a). The first three iterates are indicated by points 1, 2 and 3, respectively.

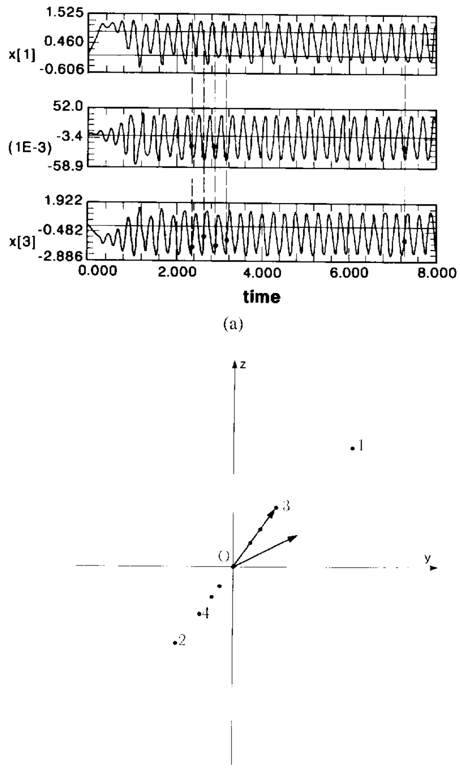


Fig. 3. (a) Waveforms associated with a stable limit cycle from Chua's circuit obtained with $\alpha = 8.1$, $\beta = 100/7$, $a = -8/7$, and $b = -5/7$. (b) Eigenvectors associated with two negative eigenvalues of the Poincaré map of the stable limit cycle of Fig. 3(a). The first four iterates are indicated by points 1, 2, 3 and 4, respectively.

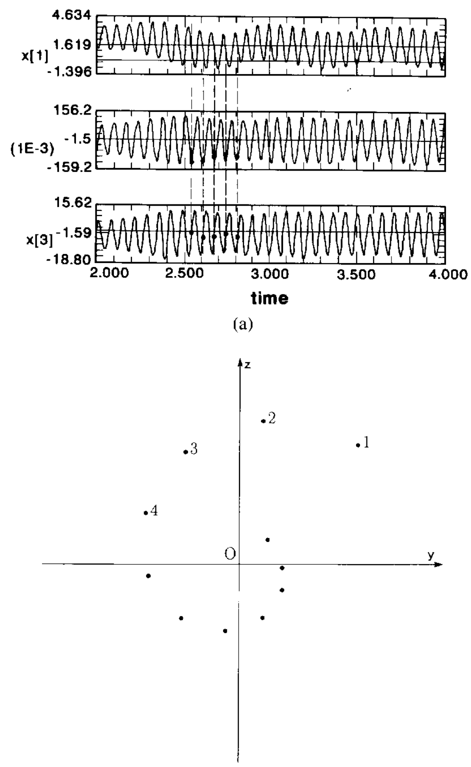


Fig. 4. (a) Waveforms associated with a stable limit cycle from Chua's circuit obtained with $\alpha = 1500$, $\beta = 10\,000$, $a = -1.026$, and $b = -0.982$. (b) Poincaré map of the stable limit cycle of Fig. 4(a), which has two complex conjugate eigenvalues. The first four iterates are indicated by points 1, 2, 3 and 4, respectively.

## III. Characteristic Multiplier Loci for Period-Doubling Sequence

Now that we know a little more about the CM, let us modify a parameter of the system and watch how the CM changes. Throughout this section, the following parameters for Chua's circuit are used: $\beta = 100/7$; $a = -8/7$; $b = -5/7$ (Fig. 5). We will vary only the parameter $\alpha$ and plot the corresponding CM (Table I) in the complex plane shown in Fig. 5.

When $\alpha$ is smaller than 6.8, the point $(1.5, 0, -1.5)$ of the state space is a stable equilibrium point (a sink). As we increase $\alpha$, this equilibrium point becomes unstable and a period-1 limit cycle is born. One of the CM's is very close to 1 and the other is close to 0. As we increase the parameter further, the larger CM decreases while the other increases. After they meet, they bifurcate into two complex conjugate values in the right-half plane, and migrate continuously into the left-half plane. Then they become both negative and real, one increases to 0 and the other decreases to $-1$. The most interesting phenomenon occurs when a CM of this limit cycle passes through $-1$. At this moment, the original (period-1) limit cycle becomes unstable, while simultaneously a stable period-2 cycle is born with a CM equal to $+1$, and remains stable as $\alpha$ increases. As we increase $\alpha$ further, we observe the same basic qualitative behavior occurs but with an ever smaller increase of $\alpha$. The CM loci for four such period-doubling bifurcations for Chua's circuit (using the above

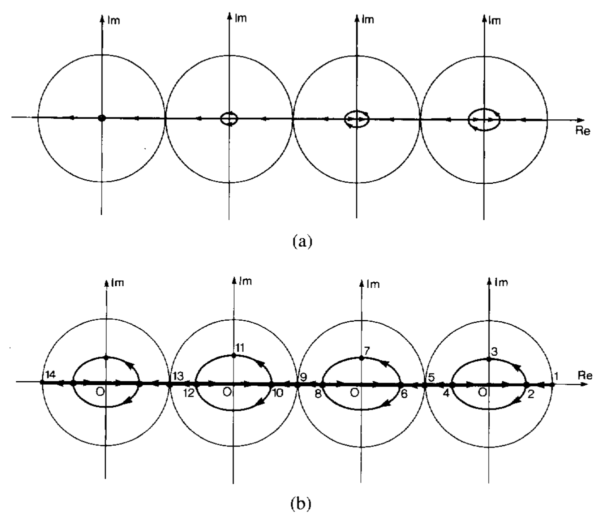


Fig. 5. (a) CM loci obtained with $\beta = 100/7$, $a = -8/7$, and $b = -5/7$ for Chua's equation corresponding to a period-1 limit cycle ($\alpha = 6.8$), which bifurcates by *period doubling* as $\alpha$ increases to $\alpha = 8.2$ (period 2), $\alpha = 8.422$ (period 4), and $\alpha = 8.45419$ (period 8). (b) Schematic CM loci redrawn (not according to scale) for the clarity of the figure.

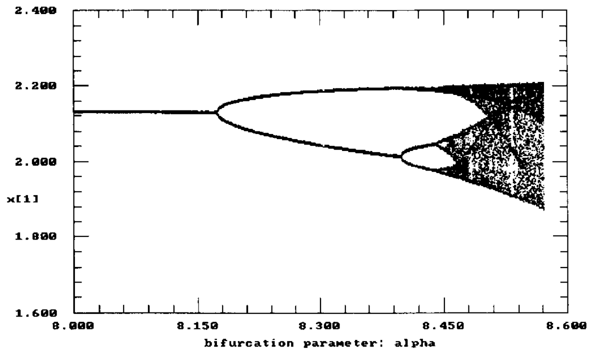


Fig. 6. Bifurcation map obtained with $\beta = 100/7$, $a = -8/7$, and $b = -5/7$ for Chua's dimensionless equation where $\alpha$ increases from 8 to 8.5.

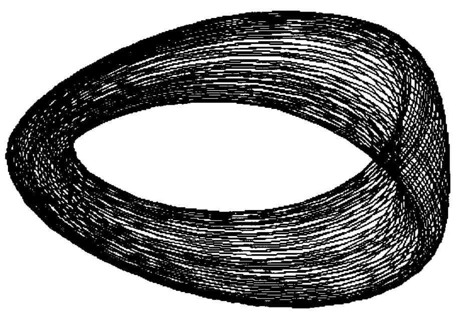

Fig. 7. Torus drawn in 3-D space obtained with $\alpha = 2000$, $\beta = 10\,000$, $a = -1.026$, and $b = -0.982$.

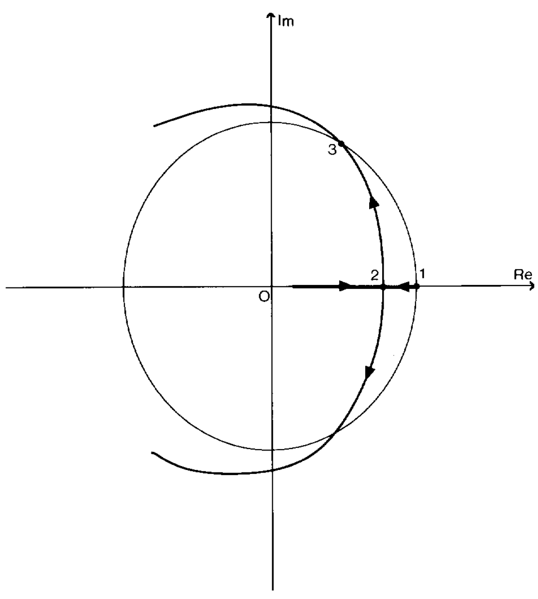


Fig. 8. CM loci obtained with $\beta = 10\,000$, $a = -1.026$, and $b = -0.982$ for Chua's circuit corresponding to a period-1 limit cycle ($\alpha = 725$) which bifurcates to a torus as $\alpha$ increases to $\alpha = 1767$.

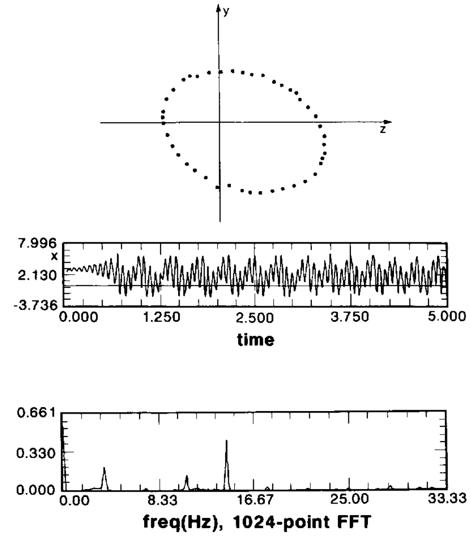


(a)

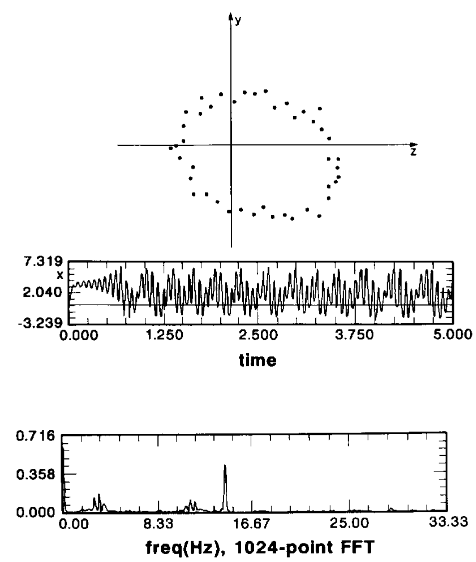


(b)

Fig. 9. Poincaré map, waveform, and frequency spectrum of $x(t)$ obtained with $\alpha = 2200$, $\beta = 10\,000$, $a = -1.04$, and $b = -0.982$. The attractor is still a torus. (b) Poincaré map, waveform, and frequency spectrum of $x(t)$ obtained with $\alpha = 2200$, $\beta = 10\,000$, $a = -1.045$, and $b = -0.982$. The attractor is almost chaotic.

fixed parameters) is plotted in Fig. 5(a). This bifurcation loci confirms the scenario described by Arnold in [8]. The relevant parameters and CM corresponding to the points indicated in Fig. 5(a) are given in Table I. Since the CM loci shrinks as we go from right to left in Fig. 5(a), we show a schematic of Fig. 5(a) (not drawn according to scale) in Fig. 5(b) where the corresponding entries in Table I are identified with their corresponding numbers.

## IV. Bifurcation Tree for Chua's Circuit

The period-doubling bifurcation phenomenon can be summarized in a graph obtained by identifying the controlling

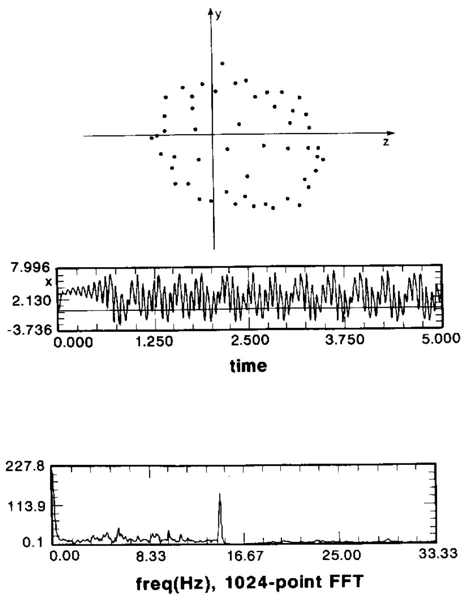


(c)

Fig. 9. (c) Poincaré map, waveform, and frequency spectrum of $x(t)$ obtained with $\alpha = 2200$, $\beta = 10\,000$, $a = -1.05$, and $b = -0.982$. The attractor is chaotic.

TABLE II
DATA FOR PLOTTING THE CM LOCI IN FIG. 8

| | $\alpha$ | CM 1 | CM 2 | Remarks |
|---|---|---|---|---|
| 1 | 725 | 0.995584 | 0.436853 | limit cycle becomes unstable as a real CM leaves the unit circle |
| | 800 | 0.906000 | 0.691892 | |
| 2 | 833 | 0.810811 | ± j 0.0150749 | CM becoming complex |
| | 1000 | 0.83885 | ± j 0.232464 | |
| | 1200 | 0.835905 | ± j 0.371101 | |
| | 1400 | 0.799179 | ± j 0.510877 | |
| | 1500 | 0.766259 | ± j 0.584179 | |
| | 1600 | 0.721792 | ± j 0.659501 | |
| 3 | 1767 | 0.616806 | ± j 0.787262 | limit cycle becomes unstable as a complex CM leaves the unit circle |
| | 1800 | 0.550785 | ± j 0.812288 | |
| | 2000 | 0.387371 | ± j 0.954079 | |

(variable) parameter ($\alpha$ in our case) as the horizontal axis and plotting all the local maxima of the steady state *periodic* waveform of one of the state coordinates along the vertical axis as shown in Fig. 6. The resulting diagram is called a *bifurcation tree*. Observe that the bifurcation (branching) points of the bifurcation tree correspond to the points on the CM loci of Fig. 5 where the CM is equal to $-1$.

## V. TRANSITION TO TORUS

Let us now investigate what happens when the CM moves out of the *complex* portion of the unit circle. In this case, we will see that the limit cycle becomes *unstable* while at the same time giving birth to a *torus*, whose associated waveforms are no longer periodic, but are *quasi-periodic*. The frequency spectrum of a torus is also very specific because it shows a finite number of sinusoidal components $\omega_1, \cdots, \omega_N$ which are incommensurable in the sense that there is no set of integers $k_1, k_2, \cdots, k_N$ (not all equal to 0) satisfying $\sum k_i\omega_i = 0$. For Chua's circuit, this occurs when the parameters are chosen as follows: $\alpha = 2000$; $\beta = 10\,000$; $a = -1.026$; $b = -0.982$ (Fig. 7).

If we keep the above parameters except $\alpha$ which we vary, we will obtain the CM loci shown in Fig. 8. The relevant parameters are summarized in Table II. As the CM approaches the unit circle (point 3) in Fig. 8, the *transients* which eventually converge to a period-1 limit cycle becomes increasingly long until it almost resembles a torus. As the CM leaves the unit circle, the steady state become a *torus.*

## VI. TORUS BREAKDOWN

Finally, we will focus our attention on the torus *breakdown.* This phenomenon occurs in Chua's equation with the following parameters: $\alpha = 2200$, $\beta = 10\,000$, and $b = -0.982$. The parameter $a$ varies from $-1.04$ to $-1.05$. The frequency spectrum of the trajectory will be our main object of discussion. When $a$ is equal to $-1.04$, the steady-state trajectory is a torus, and we can observe two incommensurate frequencies in the spectrum. While decreasing the parameter ($a = -1.045$), the two smallest frequencies split each of them into three. Although the trajectory is still a torus we are right at the boundary of chaos. While decreasing a further ($a = -1.05$), the frequency spectrum becomes a continuous curve, a phenomenon generally called *chaos.*

The waveforms of these systems are also shown in Fig. 9. It is much harder to see the difference between a torus and a chaotic attractor in this kind of diagram but still we can notice a slight change: the amplitude of the high frequency oscillation is not constant in the chaotic attractor while it is in the torus.

Observe now how the Poincaré map changes as we decrease the parameter "$a$". When "$a$" is equal to $-1.04$, the Poincaré map in Fig. 9(a) is almost an ellipse and all points lie on a 1-D curve. When "$a$" is equal to $-1.045$, the Poincaré map in Fig. 9(b) looks like that of Fig. 9(a)) in a first approximation, but some small *ears* can be seen emerging in Fig. 9(b), showing that the bifurcation to chaos is very close. Finally, when "$a$" is equal to $-1.05$, the Poincaré map in Fig. 9(c) is no longer a curve, and the points seem to wander randomly although the system is deterministic.

## REFERENCES

[1] L. O. Chua, "The genesis of Chua's circuit," *Arch. Electron. Ubertragung.*, vol. 46, no. 4, pp. 187–257, 1992.
[2] R. N. Madan (Guest Ed.), "A paradigm for chaos part I," *J. Circuits Syst. Comput.* (Special Issue on Chua's Circuit), vol. 3, no. 1, Mar. 1993.
[3] ——, "Special issue on Chua's circuit: A paradigm for chaos, Part II," *J. Circuits Syst. Comput.*, vol. 3, no. 2, June 1993.
[4] T. S. Parker and L. O. Chua, *Practical Numerical Algorithms for Chaotic Systems.* New York: Springer-Verlag, 1987.
[5] M. P. Kennedy, "Robust op amp realisation of Chua's circuit," *Frequenz*, vol. 46, no. 3–4, pp. 66–80, 1992.
[6] L. O. Chua, M. Komuro, and T. Matsumoto, "The double scroll family," *IEEE Trans. Circuits Syst.*, vol. CAS-33, pp. 1073–1118, Nov. 1986.
[7] P. Deregel, "Chua's oscillator: A zoo of attractors," (Special issue on Chua's circuit: a paradigm for Chaos, Part II), *J. Circuits Syst. Comput.*, vol. 3, no. 2, pp. 309–359, June 1993.

[8] V. I. Arnold, "Bifurcation and singularities in mathematics," in *Theoretical and Applied Mechanics* (P. Germain, M. Piau, and D. Caillerie, Eds.). Amsterdam: North-Holland, 1989, pp. 1–25.

**Laurent G. Duchesne** was born in Issy les Moulineaux, France. He received the engineering diploma from the Ecole Nationale Superieure d l'Aeronautique et de l'Espace in Toulouse, France, in 1993. He is currently studying for a Diplome d'Etudes Approfondies in Applied Mathematics.